Neurotherapeutics (2022) 19:1298–1312
https://doi.org/10.1007/s13311-022-01244-5

ORIGINAL ARTICLE

ERRγ Ligand Regulates Adult Neurogenesis and Depression-like Behavior in a LRRK2-G2019S-associated Young Female Mouse Model of Parkinson's Disease

Hyo In Kim[1] · Juhee Lim[2] · Hyo-Jung Choi[3] · Seok-Ho Kim[1] · Hyun Jin Choi[1]

Accepted: 25 April 2022 / Published online: 25 May 2022

Abstract

Adult neurogenesis, a process controlling the proliferation to maturation of newly generated neurons in the post-developmental brain, is associated with various brain functions and pathogenesis of neuropsychological diseases, such as Parkinson's disease (PD) and depression. Because orphan nuclear receptor estrogen-related receptor γ (ERRγ) plays a role in the differentiation of neuronal cells, we investigated whether an ERRγ ligand enhances adult neurogenesis and regulates depressive behavior in a LRRK2-G2019S-associated mouse model of PD. Young female LRRK2-G2019S mice (7–9 weeks old) showed depression-like behavior without dopaminergic neuronal loss in the nigrostriatal pathway nor motor dysfunction. A significant decrease in adult hippocampal neurogenesis was detected in young female LRRK2-G2019S mice, but not in comparable male mice. A synthetic ERRγ ligand, (*E*)-4-hydroxy-*N*'-(4-(phenylethynyl)benzylidene)benzohydrazide (HPB2), ameliorated depression-like behavior in young female LRRK2-G2019S mice and enhanced neurogenesis in the hippocampus, as evidenced by increases in the number of bromodeoxyuridine/neuronal nuclei-positive cells and in the intensity and number of doublecortin-positive cells in the hippocampal dentate gyrus (DG). Moreover, HPB2 significantly increased the number of spines and the number and length of dendrites in the DG of young female LRRK2-G2019S mice. Furthermore, HPB2 upregulated brain-derived neurotrophic factor (BDNF)/tropomyosin receptor kinase B (TrkB) signaling, one of the important factors regulating neurogenesis, as well as phosphorylated cAMP-response element binding protein-positive cells in the DG of young female LRRK2-G2019S mice. Together, these results suggest ERRγ as a novel therapeutic target for PD-associated depression by modulating adult neurogenesis and BDNF/TrkB signaling.

Keywords Parkinson's disease · Depression · Adult neurogenesis · BDNF · ERRγ · HPB2

Introduction

Neurogenesis is a biological process by which neuronal stem cells undergo proliferation, migration, and differentiation to form new functional neurons. Even after development, the formation, maturation, and synaptic integration of newborn neurons continue in the brain [1, 2]. Adult neurogenesis occurs in restricted areas of the human brain: subventricular zone (SVZ) of the lateral ventricle, striatum, and the subgranular zone (SGZ) of the hippocampal dentate gyrus (DG) [3]. Hippocampal neurogenesis plays a particularly important role in neuronal functions such as learning and memory, cognition, and mood regulation [4, 5]. Brain-derived neurotrophic factor (BDNF), a member of the neurotrophin family, assists the survival of hippocampal neuronal stem cells, promotes their differentiation into pyramidal-like neurons [6], and regulates granule cell neurogenesis in the DG [7]. Furthermore, BDNF/tropomyosin receptor kinase B (TrkB) downregulation in the hippocampus is associated with age-related decline in neuronal plasticity [8].

Numerous studies have shown that adult neurogenesis and BDNF are related to the pathophysiology of depression and

✉ Seok-Ho Kim
ksh3410@cha.ac.kr

✉ Hyun Jin Choi
hjchoi3@cha.ac.kr

[1] College of Pharmacy and Institute of Pharmaceutical Sciences, CHA University, Pocheon, Gyeonggi-do 11160, Republic of Korea

[2] College of Pharmacy, Woosuk University, Wanju-gun, Jeollabuk-do 55338, Republic of Korea

[3] Daegu-Gyeongbuk Medical Innovation Foundation, New Drug Development Center, Daegu 41061, Republic of Korea

antidepressant action [9–11]. Patients with major depressive disorder (MDD) not treated with antidepressants show lower granule neuron number and granular layer volume of the DG than that in treated patients [12]. Additionally, a mouse model showing reduced neurogenesis under stress conditions also shows depressive behavior [13], and chronic antidepressant treatment increases the proliferation and maturation of adult rat hippocampal neurons [14]. Moreover, brain imaging studies showing structural and functional disturbances in patients with depression also support the neurotrophic hypothesis of depression [15, 16].

Parkinson's disease (PD) is a neurodegenerative disorder characterized by a progressive loss of dopaminergic (DAergic) neurons in the substantia nigra pars compacta [17]. Although characteristic PD symptoms include motor dysfunctions, such as postural instability, bradykinesia, rigidity, and resting tremor, even diverse non-motor symptoms (NMS), such as fatigue, anxiety, depression, sleep problems, pain, constipation, and impaired olfaction, are frequently observed [18]. Depressive symptoms can appear 2–10 years before a diagnosis of PD due to abnormal movements [19]. Additionally, > 30% of patients with PD suffer from depression [20], which impacts the quality of life (QoL) [21, 22]. Furthermore, patients with a history of depression are at greater risk of PD than those without [23]. Because the pathologic mechanism of depression in patients with PD has not been fully clarified, there are no specific diagnostic criteria or treatment strategies. Recently, the survival, proliferation, and differentiation of newborn neurons in the hippocampus and SVZ/olfactory bulb system are known to be associated with depression in PD [24]. Additionally, serum BDNF levels are significantly lower in PD patients with depressive symptoms than in those without depression, and there is a negative association between the BDNF level and depression severity [25]. Thus, the regulation of adult neurogenesis and BDNF could be an attractive therapeutic target for treating depression in PD [26, 27].

Estrogen-related receptor γ (ERRγ), an orphan nuclear receptor, regulates cellular energy metabolism in various tissues (brain, skeletal muscle, and liver) [28, 29]. ERRγ is abundantly expressed in the central nervous system during development and also in the adult brain [30, 31]. In adult mice brains, ERRγ is widely expressed in the thalamus, hypothalamus, olfactory bulb, midbrain, striatum, cerebral cortex, and hippocampus [32]. Previously, we showed that ERRγ is relevant to the regulation of DAergic neuronal phenotypes [33]. Furthermore, the novel ERRγ ligand (*E*)-4-hydroxy-*N*'-(4-(phenylethynyl)benzylidene)benzohydrazide (HPB2) can enhance DAergic phenotype regulation and induce DAergic neurite outgrowth via BDNF upregulation [34].

In this study, we investigated whether ERRγ ligand HPB2 could be a novel therapeutic agent for regulating depressive behavior in a PD mouse model. For this, we used transgenic mice with the leucine-rich repeat kinase 2 (LRRK2) mutation, LRRK2-Gly2019Ser (G2019S). The phenotype of LRRK2 mutation carriers is very similar to that of patients with idiopathic PD, with PD-associated NMS (anxiety/depression-like behaviors) seen at a young age, prior to the onset of motor dysfunction [35].

Methods

Antibodies and Reagents

We used the following antibodies: mouse-anti-tyrosine hydroxylase (TH) (sc-25269), rabbit-anti-phospho-cAMP-response element binding protein (p-CREB) (sc-7989), mouse-anti-postsynaptic density protein (PSD-95) (sc-32290) (Santa Cruz Biotechnology, TX, USA); rabbit-anti-TrkB (GTX54857), rabbit-anti-BDNF (GTX132621), rabbit-anti-LRRK2 (GTX113065) (GeneTex, CA, USA); rabbit-anti-TH (ab152), rabbit-anti-neuronal nuclei (NeuN) (EPR12763) (Abcam, Cambridge, UK); mouse-anti-bromodeoxyuridine (BrdU) (MA3-071) (Thermo Fisher Scientific, MA, USA); rabbit-anti-doublecortin (DCX) (#4604), mouse-anti-α-tubulin (T6074), and mouse-anti-β-actin (A1978) (Cell Signaling Technology, MA, USA). Additionally, mouse anti-horseradish peroxide-conjugated IgG (Thermo Fisher Scientific), Alexa Fluor®-conjugated secondary antibodies (Thermo Fisher Scientific) and goat anti-rabbit biotinylated secondary antibody (Vector Laboratories, CA, USA) were used.

For in vitro cell culture, Dulbecco's modified Eagle's medium (DMEM), fetal bovine serum (FBS), and penicillin/streptomycin were obtained from Corning (NY, USA), and trypsin/ethylenediaminetetraacetic acid was from Cytiva (MA, USA). All polystyrene culture plates or dishes were purchased from Thermo Fisher Scientific.

Animals

FVB/N-Tg(LRRK2*G2019S)1Cjli/J mice expressing the human LRRK2-G2019S (GS) mutation were obtained from Jackson Laboratory (ME, USA). Through genotyping for Tg(LRRK2*G2019S)1Cjli/J, the animals were classified as either hemizygous (GS) or non-carrier (wild-type; WT). We used 7–10 weeks old mice in the experiments. All experiments were performed according to the guidelines of the Institutional Animal Care and Use Committee of the CHA University (IACUC-180059, -190095, -200073). Details can be found in the Supplementary Materials and Methods.

Treatments

HPB2 was dissolved in dimethyl sulfoxide (DMSO, Sigma-Aldrich, MO, USA). For mice injection, HPB2 solution contained 4% DMSO, 20% polyethylene glycol (PEG, Sigma-Aldrich), and 0.9% saline. Intraperitoneal (i.p.) injection was administered once daily for 17 days (excluding weekends). HPB2-treated mice were injected with 10 mg/kg HPB2, and the control mice were injected with 0.9% saline containing 4% DMSO and 20% PEG for the same duration. The administration conditions (dose, treatment duration, etc.) of HPB2 were determined based on the results of our previous study on neuronal differentiation [34]. Mice were randomly allocated into experimental groups.

For the neurogenesis analysis, mice were injected with i.p. 100 mg/kg BrdU (Sigma-Aldrich) twice daily for four consecutive days. Mice were sacrificed and perfused 14 days after the final injection. BrdU administration was performed on 8–10 weeks old mice. Furthermore, HPB2 treatment began at the same time as BrdU injection.

Analysis of LRRK2 Expression

To analyze the level of LRRK2 expression in the brain of FVB/N-Tg(LRRK2*G2019S)1Cjli/J mice, the brain was removed and dissected into olfactory bulb, cortex, striatum, substantia nigra and hippocampus, respectively. The brain tissues were homogenized and lysed with respective buffers. LRRK2 protein levels were measured by western blot analysis according to the method described below. The mRNA level of LRRK2 in each brain region was assessed by LRRK2 mRNA polymerase chain reaction (PCR) for total mRNA extracted with TRIzol™ reagent (Life Technologies, CA, USA). Details are in the Supplementary Materials and Methods.

Behavioral Tests

Forced Swim Test (FST)

The FST was used to evaluate depressive behavior. A clear glass cylinder (diameter, 18 cm; height, 26 cm) was filled up to 15 cm with water (27 ± 1 °C). Mice were gently placed in the cylinder, and the immobility time during 5 min was measured after a delay of 1 min. The movement of mice were recorded with a camera (Sony, Tokyo, Japan) in the absence of an experimenter and analyzed in an unbiased blind manner.

Tail Suspension Test (TST)

The TST was used to assess depressive behavior of mice. Each mouse was suspended in the middle of the wooden box (30 × 20 × 60 cm) by tail with adhesive tape. The distance from the mouse's nose to floor of wooden box was approximately 20–25 cm. The immobility time during 5 min was measured after a delay of 1 min. All the movements of mice were recorded with a camera (Sony) in the absence of an experimenter and analyzed in an unbiased blind manner.

Open Field Test (OFT)

The OFT was used to assess anxiety behavior. EthoVision XT9 (EthoVision®, Version 9, Wageningen, the Netherlands) and SMART video tracking systems (Version 2.5.2.1, Harvard Apparatus, MA, USA) were used to monitor the mice. Mice were individually placed in the center of an acrylic chamber (50 × 50 × 40 cm), and a video camera recorded each 10 min trial. The area excluding the center zone (25 × 25 cm) in the arena (50 × 50 cm) was set as the peripheral zone.

Light–dark Test (LDT)

The LDT was used to assess anxiety behavior. Acrylic dark (black, 10 × 30 cm) and light (white, 20 × 30 cm) chambers were divided by a partition, with a passage hole for the mouse. The duration spent in the dark chamber and the total number of transitions were recorded for 10 min. The movement of mice were recorded with a camera (Sony) in the absence of an experimenter and analyzed in an unbiased blind manner.

Rotarod Test

Motor function was assessed using a rotarod system (Rota Rod-R V2.0, B.S. Technolab, Seoul, Korea). Before the test, mice were habituated to the rod at a constant speed of 4 rpm for 3 min. The rod speed was set to accelerate from 4 to 40 rpm for 5 min. The times at which the mouse fell off the rod was automatically recorded, and the average value of three repeated trials (inter-trial interval, 20 min) was calculated.

Immunohistochemistry

Mice were anesthetized and perfused first with 0.25% heparin-phosphate buffered saline (PBS) and then with 4% paraformaldehyde. Rompun (Byer, Leverkusen, Germany; xylazine hydrochloride, sodium chloride) and Alfaxan (Jurox, NSW, Australia; alfaxalone 10 mg/ml) (mixed at 1:4) were used for anesthesia. Perfused brain tissues were frozen at -80 °C with an optimal cutting temperature compound (SAKURA Fineteck USA, CA, USA). The frozen brains were cut using a cryostat microtome (Leica, Wetzlar, Germany) at -25 °C into 20-μm thick sections. Sectioned tissues were placed on an adhesion slide (SuperFrost Plus™,

Thermo Fisher Scientific). The tissues were permeabilized, blocked, and stained, as shown in our previous study [34]. Primary antibodies used for immunohistochemistry: rabbit-anti-TH (1:400), rabbit-anti-NeuN (1:400), mouse-anti-BrdU (1:200), rabbit-anti-DCX (1:800), rabbit-anti-BDNF (1:200), rabbit-anti-p-CREB (1:400). For the neurogenesis analysis, brain tissues from BrdU-injected mice underwent 2-M hydrochloric acid hydrolysis (30 min), before primary antibody staining. Stained tissues were mounted with mounting medium (Vector Laboratories), and a coverslip was placed on the tissues. Fluorescence images were obtained using a confocal microscope (LSM 880, Carl Zeiss, Oberkochen, Germany) and captured using Zen software (Carl Zeiss). DAB images were obtained using a microscope camera (Leica). The intensity of immuno-reactivity was quantified using Image J software (NIH, MD, USA).

Western Blot Analysis

Mice brain tissues were dissected for each region and tissues were sonicated with lysis buffer. The lysis buffer contained radioimmunoprecipitation assay buffer (RIPA buffuer, 150 mM NaCl, 1% Triton X-100, 0.5% deoxycholic acid, 0.1% sodium dodecyl sulfate, 50 mM Tris–Cl, pH 7.5), protease inhibitor cocktail and phosphatase inhibitor cocktail (25×, Roche, Basel, Switzerland). Proteins were collected and quantified using Bradford protein assay reagent (Bio-Rad, CA, USA). Protein samples were separated with 8% or 12% sodium dodecyl sulfate polyacrylamide gels and transferred to polyvinylidene difluoride membranes. The following antibodies were used: mouse-anti-TH (1:4000), rabbit-anti-BDNF (1:1000), rabbit-anti-TrkB (1:1000), rabbit-anti-NeuN (1:4000), rabbit-anti-LRRK2 (1:500), mouse-anti-PSD-95 (1:1000), mouse-anti-α-tubulin (1:20,000), and mouse-anti-β-actin (1:10,000). Specific proteins were visualized using enhanced chemiluminescence detection kits (Millipore, MA, USA) and analyzed using a luminescent image analyzer (LAS-4000, GE Healthcare, Uppsala, Sweden). Alpha-tubulin and β-actin were used as loading controls. Densitometric analysis of western blotting data was performed using ImageJ software. Adobe Photoshop was used to create the immunoblot images.

Golgi-cox Staining

FD Rapid GolgiStain™ Kit (FD Neuro Technologies, Inc., MD, USA) was used on fixed-brain tissues according to the manufacturer's protocol. After the impregnation and cryoprotection steps, brain tissues were frozen at -80 ℃ in distilled water and coronally cut into 100-µm thick sections. Brain sections were mounted on gelatin-coated sides (coated with 0.5% gelatin from cold water fish skin, 0.05% chromium(III) potassium sulfate dodecahydrate and distilled water). Tissues were stained and dehydrated according to the manufacturer's protocol. Tissues were protected from light during all steps. Golgi-Cox stained images were obtained by optical microscope (Leica). The Golgi-stained dendrites were analyzed by ImageJ according to the methods previously reported [36]. Specifically, images of 25-µm dendritic segments (n = 30–36 images, 8 sections per an animal, 6 animals per a group) were skeletonized by ImageJ software, and the number of spines were calculated by independent researcher in an unbiased blind manner. Dendritic branches (n = 12 neurons, 8 sections per an animal, 6 animals per a group) were traced by NeuronJ plug-in [37] and the number and length of dendrites were analyzed by ImageJ software.

ERR Selectivity Assay

To verify the binding selectivity of ERR subtypes with HPB2 in HEK293T cells, pGL4.35[luc2P/9XGAL4UAS/Hygro] (E1370, Promega, WI, USA) and ERRs-LBD vector was utilized. Expression vectors in ERRs-LBD were generated by subcloning the LBDs (ERRα: amino acid 189–423; ERRβ: amino acid 208–433; ERRγ: amino acid 222–458) of the corresponding nuclear receptors into the pFN26A (BIND) vector (E1380, Promega). All transfection experiments were performed in HEK293T cells in Poly-D-Lysine coated 96 well plates (Corning), by using Lipofectamine2000 (Invitrogen, MA, USA) according to the manufacturer's instructions. For Dual luciferase assay, 20 ng of GAL4 construct and 20 ng of ERRα/β/γ-LBD construct were added per well. Cells were transfected for 24 h, then HPB2 was added for an additional 24 h. Dual luciferase assay was carried out using the Dual-Luciferase Reporter Assay System (E1960, Promega), and luciferase activity was analyzed according to the manufacturer's instructions. Briefly, cells were lysed with passive lysis buffer, treated with Luciferase assay buffer II, and Firefly luminescence was measured by the luminometer (SYNERGY Neo2, BioTek, VT, USA). Stop & Glo buffer was added to each well, and Renilla luminescence was measured. The ERR luciferase activities were indicated by normalizing Firefly luciferase activity to Renilla luciferase activity in each sample.

Analysis of BDNF Levels in HT22 Cells

BDNF expression levels in hippocampal neuronal cell line HT22 cells were evaluated by quantitative reverse transcription-PCR (qRT-PCR) and immunocytochemistry. Details about HT22 cell culture and the experiments can be found in the Supplementary Materials and Methods.

Data Analysis

All data are displayed as the mean ± standard error of mean (SEM). To compare each group, we performed one-way analysis of variance (ANOVA) with Bonferroni's multiple comparison test (when F was significant [$p < 0.05$] and there was no variance inhomogeneity), or unpaired t-test, using Prism software (GraphPad, CA, USA). For behavioral analyses, data were averaged after excluding the highest and lowest values. The size for each experimental group was approximately same. *P*-values of $*p < 0.05$, $**p < 0.01$, $***p < 0.001$, and $****p < 0.0001$ were considered statistically significant.

Results

Young Female LRRK2-G2019S Mice Show Depressive Behavior

We previously showed significant motor deficiency and decreased nigrostriatal TH levels in old-age mice expressing the LRRK2-G2019S (GS) mutation (B6;C3-Tg(PDGFB-LRRK2*G2019S)340Djmo/J) in a PD mouse model [38]. Specifically, depression-like and anxiety-like behaviors were shown in the middle-aged group (43–52 weeks) prior to the onset of PD-like motor deficits. In this study, we used FVB/N-Tg(LRRK2*G2019S)1Cjli/J mice to further verify whether the GS mutation is involved in the occurrence of PD-associated NMSs and is associated with abnormal hippocampal neurogenesis. Because an age-dependent reduction in striatal dopamine content, significant neural degeneration, and characteristic motor dysfunction appeared in FVB/N-Tg(LRRK2*G2019S)1Cjli/J mice after 12 months of age, they are widely used to study PD pathology [39].

We first identified that LRRK2 was broadly expressed in various brain regions of FVB/N-Tg(LRRK2*G2019S)1Cjli/J mice, including the olfactory bulb, cortex, striatum, substantia nigra and hippocampus (Supplementary Fig. 1). Especially, higher LRRK2 protein levels were detected in the cortex, striatum and hippocampus, than other brain regions (Supplementary Fig. 1a-d). Brain LRRK2 expression patterns were not significantly different between male and female, or WT and GS brain, respectively. We also confirmed that human transgene LRRK2 mRNA was detected only in the GS group not in the WT (Supplementary Fig. 1e–f).

Here, we evaluated depressive and anxiety behaviors to determine the NMS phenotype in GS mice aged 7–9 weeks. We compared the behavioral results between WT and GS groups in male and female groups, respectively (Fig. 1a). In females, the immobility time on the FST and TST was longer (suggesting increased depressive behavior) in the GS group than in the WT group (Fig. 1b–c). However, in males, there were no differences in immobility times between WT and GS groups (Fig. 1d–e). In both male and female mice, there were no differences between WT and GS groups in the total distance and duration in the peripheral zone on the OFT, as well as the duration in the dark chamber and number of transitions on the LDT (Fig. 1f–m). These results indicate that depressive behavior is increased in young GS mice in a sex-dependent manner.

Hippocampal Neurogenesis is Reduced in Young Female LRRK2-G2019S Mice, Without a Decrease in Nigrostriatal TH Expression

After completing the behavioral tests, mice were sacrificed to examine the brain pathology (Fig. 1a). We evaluated the nigrostriatal DAergic neuronal degeneration (characteristic in PD) by measuring TH-immunoreactivity of the striatum and substantia nigra on immunohistochemistry and western blots. In both male and female mice, there were no significant differences between WT and GS groups in TH intensity and protein expression in the striatum and substantia nigra (Fig. 2a–h). These results suggest that young female mice with the GS mutation exhibit depressive behavior before there is a detectable loss of DAergic neurons in the nigrostriatal pathway.

GS mice show decreased survival and proliferation of newly generated neurons in the DG and neurite outgrowth inhibition [40]; moreover, reduced hippocampal adult neurogenesis is noted in depression and PD animal models [12, 13, 41, 42]. Therefore, we examined whether impaired adult neurogenesis is associated with depressive behavior in young female GS mice. The neurogenesis in the SGZ of the DG were verified by counting BrdU-positive and NeuN-positive cells. In female mice (Fig. 2i–k), the numbers of both BrdU-positive and BrdU/NeuN-positive neurons were significantly lower in GS mice than in WT mice, suggestive of reduced neuronal survival and maturation. In male mice (Fig. 2l–n), there was no difference in the number of BrdU-positive cells between WT and GS groups ($p = 0.6495$). Although the number of BrdU/NeuN-positive neurons tended to be lower in male GS mice than in WT mice, the difference was not significant ($p = 0.0629$). These results indicate that adult neurogenesis is inhibited in young female GS mice, which also shows depressive behavior.

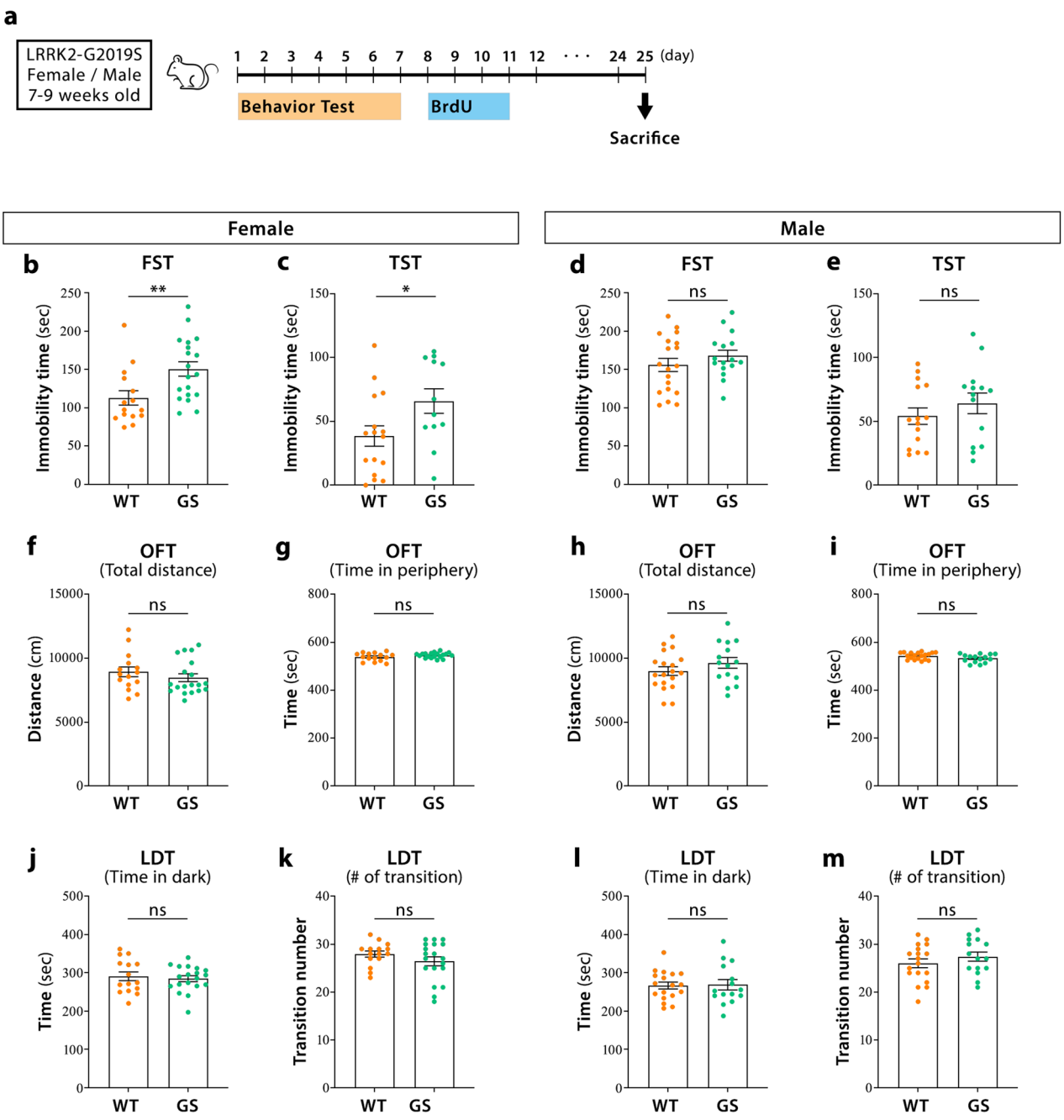

Fig. 1 Depression-like behaviors in young female LRRK2-G2019S mice. (**a**) Timing of the behavioral tests and BrdU injections. (**b-m**) All behavioral analyses were performed separately in female and male mice. The GS group was compared to the WT group ($n \geq 12$). (**b, d**) Immobility time on the FST. (**c, e**) Immobility time on the TST. (**f, h**) Total distance on the OFT. (**g, i**) Time in the periphery on the OFT. (**j, l**) Time in the dark chamber on the LDT. (**k, m**) Number of transitions on the LDT. All data are shown as the mean ± standard error of the mean. $*p < 0.05$ and $**p < 0.01$; ns, not significant; LRRK2, leucine-rich repeat kinase 2; BrdU, bromodeoxyuridine; FST, forced swim test; TST, tail suspension test; OFT, open field test; LDT, light–dark test; WT, wild-type; GS, LRRK2-G2019S

ERRγ Ligand HPB2 Improves Depressive Behavior and Adult Neurogenesis in Female LRRK2-G2019S Mice

Our previous study [34] showed that ERRγ ligand HPB2 improves neuronal outgrowth and DAergic neuronal phenotype via BDNF upregulation in vitro and in vivo (i.p. injection of 10 mg/kg HPB2 for 17 days was effective for neuronal differentiation). Because BDNF plays an important role in the maturation and synapse integration of newborn neurons in adult neurogenesis [43], here we evaluated whether HPB2 enhances hippocampal neurogenesis and regulates depressive behavior of GS mice.

The effect of HPB2 on depressive behavior in young female GS mice was evaluated using the FST (Fig. 3a). HPB2 did not significantly influence body weight in both WT and GS groups (Fig. 3b). In the GS group, the immobility time on the FST was significantly lower in HPB2-treated mice than in non-treated mice (Fig. 3c). In the WT group, the immobility time was also decreased by HPB2, but the difference was not statistically significant ($p = 0.2008$). Additionally, there were no significant differences in motor function on the rotarod test among all groups (Fig. 3d). These results indicate that HPB2 ameliorates depressive behavior in young female GS mice.

To verify the effect of HPB2 on neurogenesis, HPB2 was injected for 17 days, along with BrdU for the first 4 days (Fig. 3e). In the WT group, HPB2 had no effect; in the GS group, HPB2 restored the survival and maturation of BrdU-positive newborn neurons to a level comparable to that of WT control mice (Fig. 3f–h). These results indicate that decreased adult neurogenesis in GS mice can be restored with HPB2 administration.

HPB2 Increases the Number of DCX-positive Cells and Dendritic Spines in the DG

We next evaluated the effect of HPB2 on DCX expression, a marker of immature neurons, in the DG of young female GS mice. DCX is used as an indicator of the process of the active generation and growing of newborn neurons [44]. DCX is associated with neuronal migration during development [45] and is related to neurite outgrowth [46]. The number of DCX-positive cells and DCX intensity in the DG were significantly lower in GS mice than in WT mice (Fig. 4a–c). However, HPB2 restored the reduced DCX expression in GS mice to the level of WT control mice. Additionally, the number and length of neurites were reduced in GS mice but enhanced by HPB2 in both WT and GS mice (Fig. 4a). Furthermore, the spine number, dendritic length, and the number of dendrites of hippocampal neurons were diminished in GS mice than in WT mice (Fig. 4d–g). However, HPB2 increased the number of spines and dendrites, and induced dendritic elongation. Also, HPB2 upregulated the expression of PSD-95, a regulator of synaptic plasticity and transmission [47], in the hippocampus of GS mice (Supplementary Fig. 2). Therefore, HPB2 may induce morphological and functional maturation of newborn neurons in the DG of female GS mice.

HPB2 Promotes the BDNF/TrkB Signaling Pathway in the Hippocampus

Because our previous study [34] showed that HPB2 increases BDNF/TrkB in neuronal cells, we asked whether the effect of HPB2 on BDNF expression was comparable to that of fluoxetine using the hippocampal neuronal cell line HT22 cells. Fluoxetine, a selective serotonin reuptake inhibitor, is used to treat MDD and regulates neurogenesis and BDNF [48]. In HPB2-treated HT22 cells, BDNF mRNA levels were significantly upregulated compared to control cells, which was even higher than cells treated with fluoxetine (Supplementary Fig. 3a). Additionally, on immunocytochemistry, HPB2 increased BDNF intensity in HT22 cells (Supplementary Fig. 3b, c).

We then examined whether BDNF signaling was upregulated by HPB2 in the hippocampus of female GS mice. BDNF and BDNF receptor TrkB expression levels were lower in GS mice than in WT mice; HPB2 restored this reduced expression to similar or higher levels than those of non-treated WT mice (Fig. 5a–f). There were no significant differences in BDNF and TrkB levels between non-treated and HPB2-treated WT mice. To determine whether the difference in the levels of BDNF and TrkB between groups could be a result of the difference in neuronal damage, we evaluated the expression level of NeuN as a mature neuronal marker. As shown in Fig. 5a, d, there were no differences among all groups. Furthermore, HPB2-induced upregulation of BDNF was observed in the substantia nigra of young female GS mice, but not in WT mice (Supplementary Fig. 4).

We also measured p-CREB at Ser133, which is an active form of CREB and plays a crucial role in BDNF protein transcription [49], in the SGZ. The number of p-CREB-positive SGZ cells was markedly lower in GS mice than in WT mice. However, HPB2 recovered the number of p-CREB-positive cells to a level similar to that of WT control mice (Fig. 5g–h). These results indicate that HPB2 enhances BDNF/TrkB and p-CREB expression in hippocampal neurons in young female GS mice.

HPB2 Selectively Binds with ERRγ

In previous study [34], we showed that HPB2 directly bound ERRγ with high affinity by molecular docking study and ERRγ-LBD luciferase assay. Furthermore, the interaction of

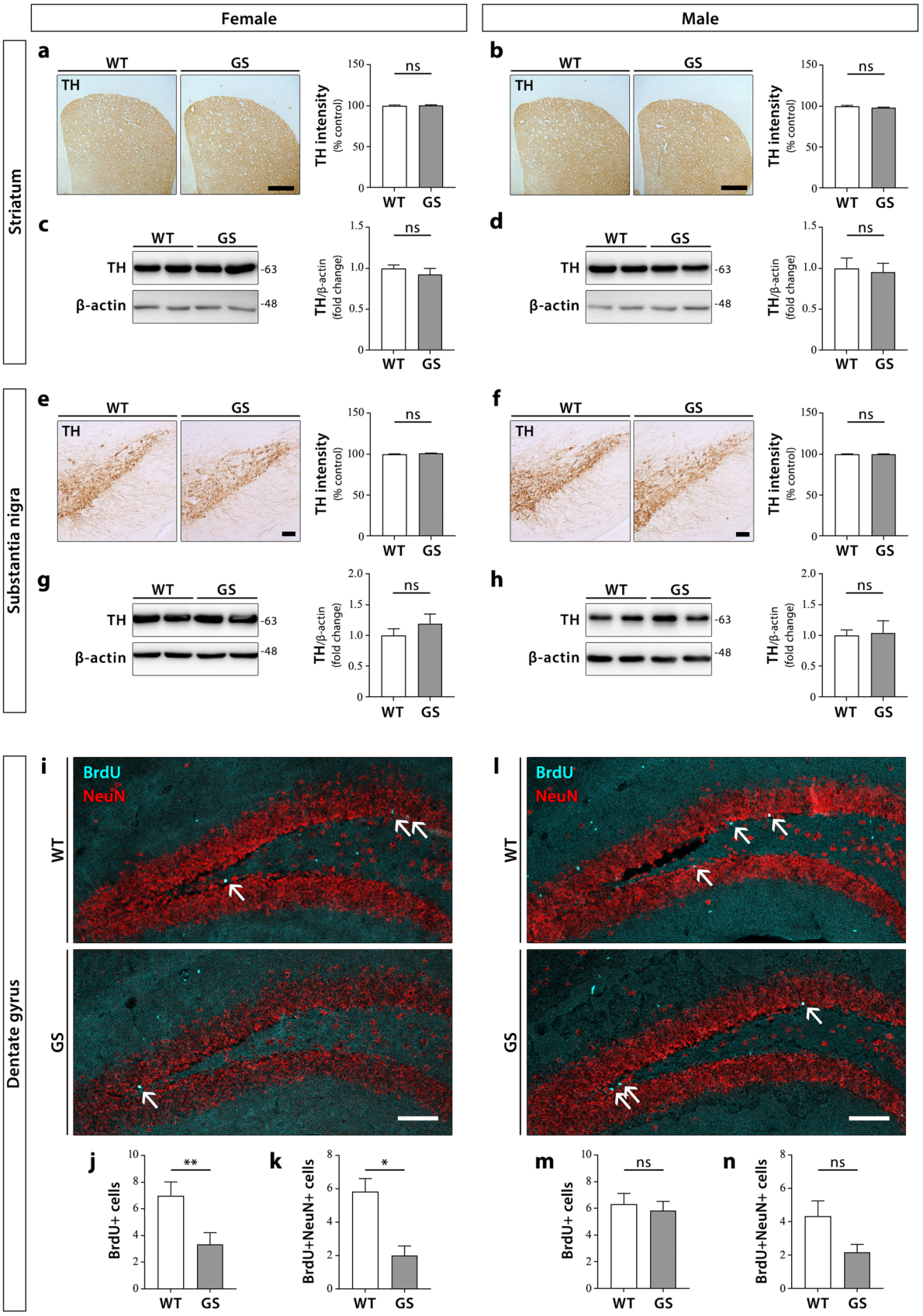
Female
Male
Striatum
Substantia nigra
Dentate gyrus
a
b
c
d
e
f
g
h
i
l
j
k
m
n
WT
GS
TH
β-actin
-63
-48
ns
TH intensity (% control)
TH/β-actin (fold change)
BrdU
NeuN
BrdU+ cells
BrdU+NeuN+ cells
**
*

◂**Fig. 2** Nigrostriatal DAergic neuronal loss and hippocampal neurogenesis in young LRRK2-G2019S mice. (**a–n**) All experiments were performed separately in female and male mice. The GS group was compared to the WT group. (**a, b**) TH-immunohistochemistry in the striatum (n = 6); scale bar = 500 μm. (**c, d**) Western blot analysis shows the TH expression in the striatum (n = 6). (**e, f**) TH-immunohistochemistry in the substantia nigra pars compacta (n = 6); scale bar = 100 μm. (**g, h**) Western blot analysis shows the TH expression in the substantia nigra (n = 6). (**i-n**) Immunofluorescence staining of BrdU (cyan) and NeuN (red) in the hippocampus dentate gyrus. The numbers of BrdU- and BrdU/NeuN-positive cells were counted and compared between groups (n = 6); scale bar = 100 μm. All data are shown as the mean ± standard error of the mean and the n throughout the data indicates the number of animals. $*p < 0.05$ and $**p < 0.01$; ns, not significant; WT, wild-type; GS, LRRK2-G2019S; TH, tyrosine hydroxylase; BrdU, bromodeoxyuridine; NeuN, neuronal nuclei

HPB2 and ERRγ regulated BDNF expression and relevant signals. Here, we further confirmed whether the binding of HPB2 to ERRγ was more selective than other ERRs. We compared the effect of HPB2 on transcriptional activity of ERRα, β and γ to identify the ERRγ selectivity of HPB2 (Fig. 6). HPB2 showed concentration-dependent upregulation only in ERRγ luciferase activity, but not in ERRα and β luciferase activity. More interestingly, the ratio of luciferase activity of ERRγ to ERRβ in HPB2-treated HEK293T cells was more than doubled with increasing concentration of HPB2, whereas GSK4716, a compound reported as an ERRβ/γ agonist, showed a ratio of nearly 1 (Table 1). These results suggest that HPB2 has a ERRγ binding selectivity over ERRα or β.

Discussion

BDNF is the most representative neurotrophin involved in the regulation of neurogenesis, and its modulation may be an attractive therapeutic strategy for depression. However, little is known about the molecular targets that can modulate BDNF signaling pathways. In the present study, we demonstrated that the novel ERRγ ligand HPB2 upregulates BDNF/TrkB signaling, which improves adult neurogenesis and depression-like behavior in a GS-associated young female mouse model of PD.

Although BDNF is associated with the pathophysiology of depression, limitations remain in the clinical application of therapeutics against depression. The application of the BDNF protein itself as an antidepressant has been unsuccessful because of its short in vivo half-life (due to instability) and low bioavailability (due to poor blood–brain barrier permeability) [50]. In a rodent depression model, a single BDNF protein infusion into the hippocampus ameliorated depressive behavior, but the antidepressant effect lasted only 3 days [51]. Another strategy involves small molecules that directly activate the TrkB signaling pathway. For example, small molecules that regulate the TrkB, including dimeric peptides, were designed as clinically useful neurotrophic drugs [52–54]. TrkB ligand small molecules can reduce the immobility time in depressed mice, but do not regulate BDNF or synaptogenesis [55]. Small molecules that directly regulate BDNF expression may also be an attractive candidate for regulating depression. Although current antidepressants that act on the monoaminergic system increase brain BDNF expression to some extent, identification of novel targets regulating central BDNF expression could provide an alternative treatment approach to overcome the limitations of current antidepressants.

In our previous study [34], HPB2 bound to ERRγ and modulated BDNF signaling and the DAergic neuronal phenotype. HPB2-induced activation of extracellular-signal-regulated kinase (ERK)-CREB signaling was relevant to the increase in BDNF. In the present study, HPB2 markedly stimulated BDNF/TrkB and p-CREB expression in the DG (Fig. 5). Consequently, HPB2 attenuated depressive behavior in female GS mice (Fig. 3). A clinical study reported that serum BDNF levels were decreased in PD patients with depression, especially in female [56]. These results imply that decreased neurotrophic signaling affected adult neurogenesis in female GS mice, and the antidepressant-like effect of HPB2 was specific to the pathological condition. In this study, the effect of HPB2 on BDNF expression was not detected in the brain of WT female mice, unlike the results in the in vitro HT22 culture system. The reason why the effect of HPB2 on BDNF expression is not seen in WT female mice brain is currently unclear, but we cannot rule out the possibility that estrogen in female mice might affect the ERR activation. ERR family are similar in the sequence homologies with estrogen receptor (ER) family, and they share the target genes and co-regulators [57]. ERR family also binds to estrogen response element (ERE), and directly and indirectly interferes with estrogen response [58, 59]. Remarkably, estrogen can upregulate BDNF transcription in brain, as binding a sequence similar to ERE of *bdnf* gene [60]. In females, other factors including estrogen affect the regulation of BDNF, and therefore, it is presumed that the BDNF upregulation by ERR ligand HPB2 also shows a difference between WT and GS.

The LRRK2 mutation is a frequent cause of genetic and sporadic PD [61]. In this study, sex differences were observed in the brain pathology and depressive behaviors of GS mice. Although motor function was not impaired in both young male and female GS mice, increased depressive behavior (Fig. 1) and decreased hippocampal neurogenesis

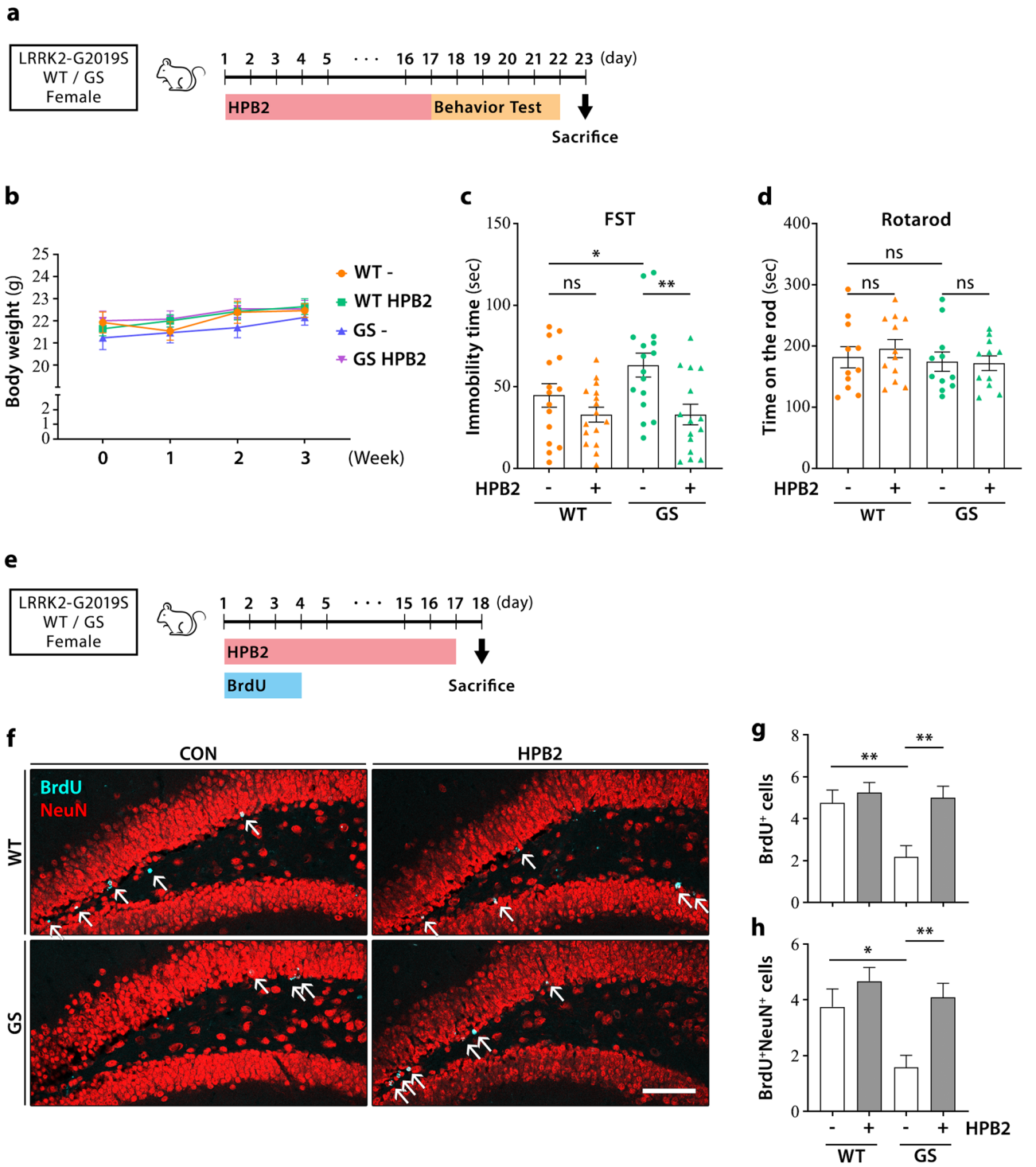

Fig. 3 Depressive behavior and adult neurogenesis were regulated by HPB2 in young female LRRK2-G2019S mice. (**a**) Timing of HPB2 injections for the behavior tests. (**b**) Body weight changes during injection and the experiments (n = 13). (**c**) Immobility time on the FST (n ≥ 15). (**d**) Time on the rod in the rotarod test (n ≥ 11). (**e**) Timing of HPB2 injections for the neurogenesis experiment. (**f–h**) Immunofluorescence staining of BrdU (cyan) and NeuN (red) in the hippocampus dentate gyrus; scale bar = 100 μm. The numbers of BrdU-positive (**g**) and BrdU/NeuN co-stained (**h**) cells were counted and compared between groups (n = 12). All data are shown as the mean ± standard error of the mean and the n throughout the data indicates the number of animals. *$p < 0.05$ and **$p < 0.01$; ns, not significant; LRRK2, leucine-rich repeat kinase 2; WT, wild-type; GS, LRRK2-G2019S; CON, control; HPB2, (*E*)-4-hydroxy-*N*'-(4-(phenylethynyl)benzylidene)benzohydrazide; FST, forced swim test; BrdU, bromodeoxyuridine; NeuN, neuronal nuclei

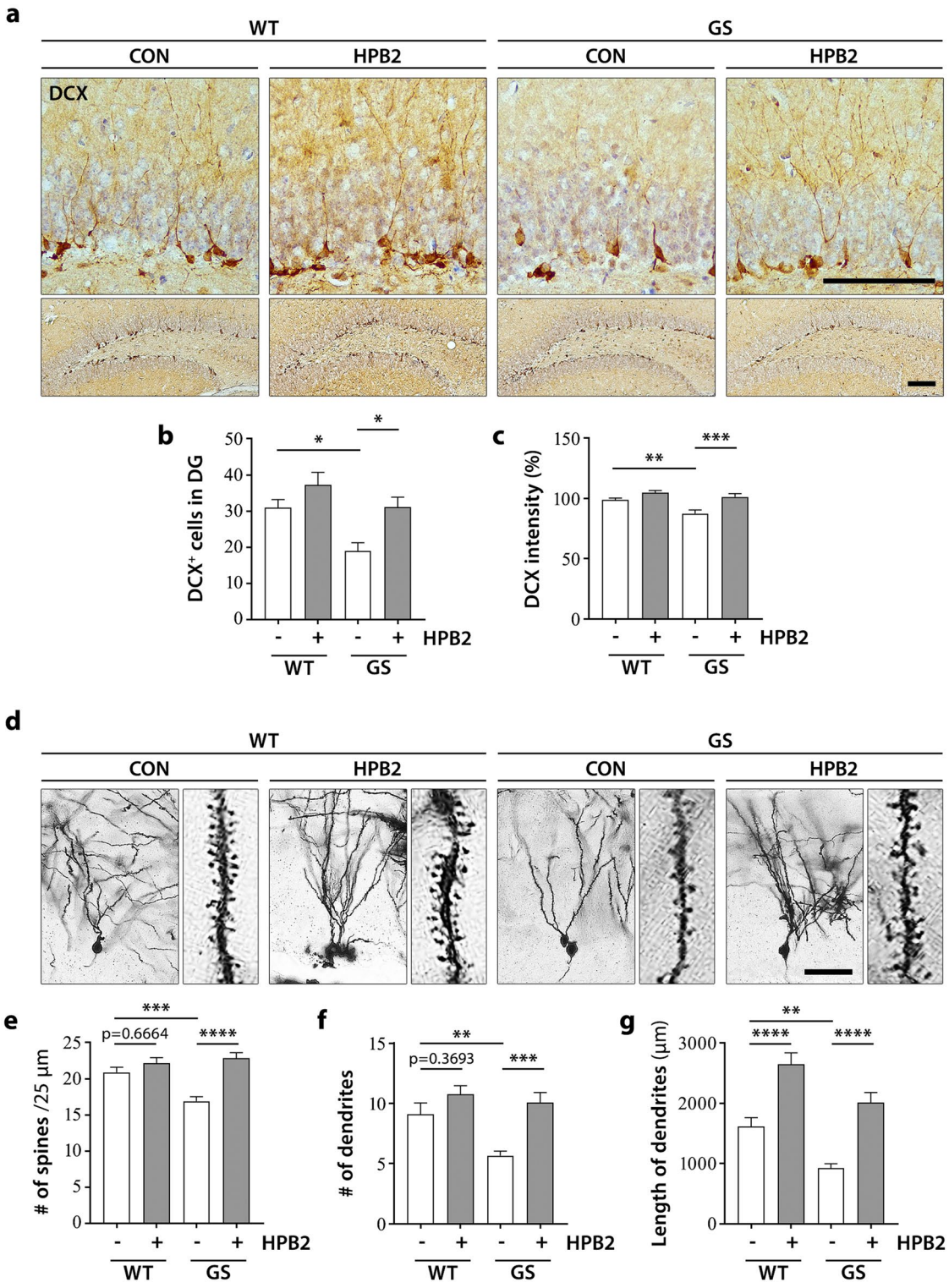

Fig. 4 HPB2 promoted DCX expression and neuronal outgrowth of DG granule neurons in young female LRRK2-G2019S mice. (**a–c**) DCX immunohistochemistry in the DG (brown: DCX, violet: nucleus); scale bar = 100 µm. (**b**) Number of DCX positive cells in the DG (n ≥ 10 animals). (**c**) DCX intensity in granular neurons (n ≥ 10 animals). (**d–g**) Golgi-Cox staining of granule neurons and the dendritic spines in the DG. (**e**) The number of spines in 25-µm dendrites was counted (n = 30–36 images). (**f, g**) The number and the length of dendrites in granule neurons (n = 12 neurons); scale bar = 50 µm. All data are shown as the mean ± standard error of the mean. $*p < 0.05$, $**p < 0.01$, $***p < 0.001$, $****p < 0.0001$; WT, wild-type; GS, LRRK2-G2019S; DCX, doublecortin; DG, dentate gyrus; CON, control; HPB2, (*E*)-4-hydroxy-*N*'-(4-(phenylethynyl) benzylidene)benzohydrazide

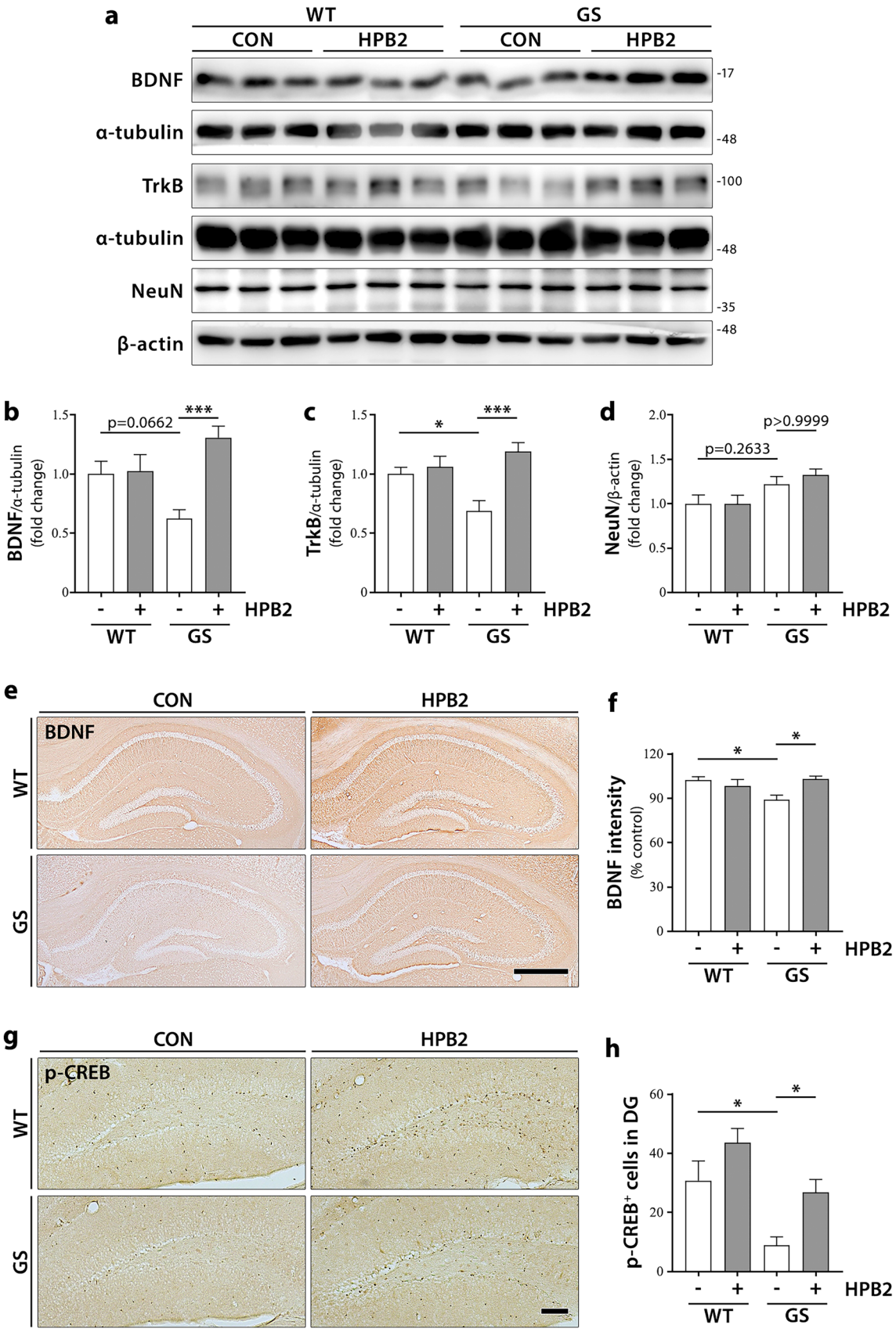
a
WT
GS
CON
HPB2
CON
HPB2
BDNF
α-tubulin
TrkB
α-tubulin
NeuN
β-actin
-17
-48
-100
-48
-35
-48
b
BDNF/α-tubulin (fold change)
p=0.0662
***
HPB2
WT
GS
c
TrkB/α-tubulin (fold change)
*
***
d
NeuN/β-actin (fold change)
p>0.9999
p=0.2633
e
CON
HPB2
BDNF
WT
GS
f
BDNF intensity (% control)
g
p-CREB
h
p-CREB+ cells in DG

◂**Fig. 5** HPB2 upregulated BDNF/TrkB and p-CREB expression in the hippocampus of young female LRRK2-G2019S mice. (**a–d**) Western blot analysis shows BDNF, TrkB and NeuN expression in the hippocampus. Alpha-tubulin and β-actin were loading controls. Data were quantified using densitometric analysis (n = 6 animals). (**e, f**) Immunohistochemistry of BDNF and BDNF intensity in the hippocampus (n ≥ 6 animals); scale bar = 500 μm. (**g, h**) Immunohistochemistry of p-CREB and p-CREB-positive cells were counted in the DG (n ≥ 10 animals); scale bar = 100 μm. All data are shown as the mean ± standard error of the mean. *$p < 0.05$, ***$p < 0.001$; WT, wild-type; GS, LRRK2-G2019S; CON, control; HPB2, (*E*)-4-hydroxy-*N*'-(4-(phenylethynyl)benzylidene)benzohydrazide; BDNF, brain-derived neurotrophic factor; TrkB, tropomyosin receptor kinase B; NeuN, neuronal nuclei; CREB, cAMP-response element binding protein; DG, dentate gyrus

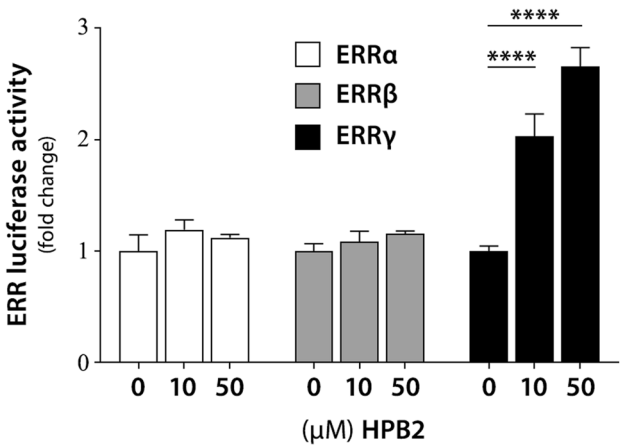

Fig. 6 ERR selectivity assay. Luciferase activities of ERRα, ERRβ and ERRγ were measured using a reporter gene assay (n = 6). Cells were treated with indicated concentration of HPB2 for a day. Data are shown as the mean ± standard error of the mean. ****$p < 0.0001$. ERR, estrogen-related receptor; HPB2, (*E*)-4-hydroxy-*N*'-(4-(phenylethynyl)benzylidene)benzohydrazide

(Fig. 2) were only detected in female GS mice. The underlying mechanism for these pathological and behavioral sex differences was not evaluated. Among patients with familial PD, GS carriers show a higher rate of depression than that in non-carriers [62], as well as a more prominent evolution in depression symptoms during a 2-year follow-up study [63]. Additionally, several studies have showed higher prevalence of depression in female patients with PD [64]. In fact, PD-related depression is more common in female GS carriers [65]. Sex differences in NMS can also be applied as a crucial diagnostic indicator.

Although the pathological mechanism by which the LRRK2 mutation modulates neurogenesis is unclear at present, several studies provide new insights regarding its association with neurogenesis regulatory signals. LRRK2 is expressed during development [66], and plays an essential role in the generation and maturation of neuronal synapses [67]. It is of interest that a significant decrease in hippocampal neurogenesis was detected in GS mice also exhibiting depressive behavior, which were ameliorated by ERRγ ligand HPB2 (Fig. 3). Furthermore, HPB2 enhanced the spine number and dendritic length (a marker of synapse plasticity) of hippocampal neurons and stimulated neuronal outgrowth in hippocampal granule neurons (Fig. 4). Dendrite spines regulate brain connectivity and therefore, are major site for processing information in the brain [68]. The present study is the first to show that the GS mutation is associated with a sex-dependent expression of depression-like behavior, which is accompanied by a downregulation in neurogenesis, spine number, and dendritic length. Because BDNF is closely related to the entire neuronal life cycle [69], BDNF signaling pathway activity could regulate dendritic spines and neuronal synaptic plasticity [43]. Similar to its effect on BDNF levels, HPB2 increased PSD-95 expression in the hippocampus of young female GS mice (Supplementary Fig. 2). These results verify that HPB2, a small molecule upregulating BDNF, contributes to synapse formation and dendritic outgrowth.

In conclusion, the present study results demonstrate that ERRγ plays a role in the regulation of BDNF/TrkB pathway signaling and neurogenesis in the hippocampus, and that ERRγ ligand HPB2 has potential in ameliorating dysregulated neurogenesis and depressive behavior. Thus, ERRγ could be a new therapeutic target for regulating PD-associated NMS, such as depression, prior to the onset of motor dysfunction.

Table 1 In vitro ERR selectivity

Compound	Structure	Concentration (μM)	ERRγ/ERRβ luciferase activity ratio
GSK4716	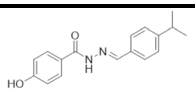	1	0.96 ± 0.05
		10	1.06 ± 0.02
HPB2	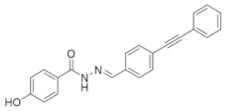	1	1.29 ± 0.07
		10	1.86 ± 0.19
		50	2.29 ± 0.15

Supplementary Information The online version contains supplementary material available at https://doi.org/10.1007/s13311-022-01244-5.

Acknowledgements This work was supported by the Basic Science Research Program through the National Research Foundation of Korea (NRF) funded by the Ministry of Science, ICT & Future Planning [NRF2021R1A2C1013180] and the Ministry of Education [NRF2021R1I1A1A01046171]; and the GRRC program of Gyeonggi Province [GRRC-CHA2017-A01, Validity and Safety Evaluation of Regional Specialized Resources]. HPB2 was synthesized and provided by Soek-Ho Kim (CHA University, Gyeonggi-do, Korea) for the experiments.

Required Author Forms Disclosure forms provided by the authors are available with the online version of this article.

References

1. Altman J, Das GD. Autoradiographic and histological evidence of postnatal hippocampal neurogenesis in rats. J Comp Neurol. 1965;124(3):319–35.
2. Gross CG. Neurogenesis in the adult brain: death of a dogma. Nat Rev Neurosci. 2000;1(1):67–73.
3. Ernst A, Frisén J. Adult neurogenesis in humans- common and unique traits in mammals. PLoS Biol. 2015;13(1): e1002045.
4. Deng W, Aimone JB, Gage FH. New neurons and new memories: how does adult hippocampal neurogenesis affect learning and memory? Nat Rev Neurosci. 2010;11(5):339–50.
5. Anacker C, Hen R. Adult hippocampal neurogenesis and cognitive flexibility - linking memory and mood. Nat Rev Neurosci. 2017;18(6):335–46.
6. Shetty AK, Turner DA. In vitro survival and differentiation of neurons derived from epidermal growth factor-responsive postnatal hippocampal stem cells: inducing effects of brain-derived neurotrophic factor. J Neurobiol. 1998;35(4):395–425.
7. Scharfman H, Goodman J, Macleod A, et al. Increased neurogenesis and the ectopic granule cells after intrahippocampal BDNF infusion in adult rats. Exp Neurol. 2005;192(2):348–56.
8. Silhol M, Bonnichon V, Rage F, Tapia-Arancibia L. Age-related changes in brain-derived neurotrophic factor and tyrosine kinase receptor isoforms in the hippocampus and hypothalamus in male rats. Neuroscience. 2005;132(3):613–24.
9. Malberg JE. Implications of adult hippocampal neurogenesis in antidepressant action. J Psychiatry Neurosci. 2004;29(3):196–205.
10. Schmidt HD, Duman RS. The role of neurotrophic factors in adult hippocampal neurogenesis, antidepressant treatments and animal models of depressive-like behavior. Behav Pharmacol. 2007;18(5–6):391–418.
11. Tanti A, Belzung C. Hippocampal neurogenesis: a biomarker for depression or antidepressant effects? Methodological considerations and perspectives for future research. Cell Tissue Res. 2013;354(1):203–19.
12. Boldrini M, Santiago AN, Hen R, et al. Hippocampal granule neuron number and dentate gyrus volume in antidepressant-treated and untreated major depression. Neuropsychopharmacology. 2013;38(6):1068–77.
13. Snyder JS, Soumier A, Brewer M, Pickel J, Cameron HA. Adult hippocampal neurogenesis buffers stress responses and depressive behaviour. Nature. 2011;476(7361):458–61.
14. Malberg JE, Eisch AJ, Nestler EJ, Duman RS. Chronic antidepressant treatment increases neurogenesis in adult rat hippocampus. J Neurosci. 2000;20(24):9104–10.
15. Duman RS, Monteggia LM. A neurotrophic model for stress-related mood disorders. Biol Psychiatry. 2006;59(12):1116–27.
16. Krishnan V, Nestler EJ. The molecular neurobiology of depression. Nature. 2008;455(7215):894–902.
17. Fahn S. Description of Parkinson's disease as a clinical syndrome. Ann N Y Acad Sci. 2003;991:1–14.
18. Barone P, Antonini A, Colosimo C, et al. The PRIAMO study: A multicenter assessment of nonmotor symptoms and their impact on quality of life in Parkinson's disease. Mov Disord. 2009;24(11):1641–9.
19. Pont-Sunyer C, Hotter A, Gaig C, et al. The onset of nonmotor symptoms in Parkinson's disease (the ONSET PD study). Mov Disord. 2015;30(2):229–37.
20. Schrag A, Ben-Shlomo Y, Quinn N. How common are complications of Parkinson's disease? J Neurol. 2002;249(4):419–23.
21. Martinez-Martin P. The importance of non-motor disturbances to quality of life in Parkinson's disease. J Neurol Sci. 2011;310(1–2):12–6.
22. Bang Y, Lim J, Choi HJ. Recent advances in the pathology of prodromal non-motor symptoms olfactory deficit and depression in Parkinson's disease: clues to early diagnosis and effective treatment. Arch Pharm Res. 2021;44(6):588–604.
23. Leentjens AF, Van den Akker M, Metsemakers JF, Lousberg R, Verhey FR. Higher incidence of depression preceding the onset of Parkinson's disease: a register study. Mov Disord. 2003;18(4):414–8.
24. Regensburger M, Prots I, Winner B. Adult hippocampal neurogenesis in Parkinson's disease: impact on neuronal survival and plasticity. Neural Plast. 2014;2014: 454696.
25. Wang Y, Liu H, Du XD, et al. Association of low serum BDNF with depression in patients with Parkinson's disease. Parkinsonism Relat Disord. 2017;41:73–8.
26. Lim J, Bang Y, Choi HJ. Abnormal hippocampal neurogenesis in Parkinson's disease: relevance to a new therapeutic target for depression with Parkinson's disease. Arch Pharm Res. 2018;41(10):943–54.
27. Lim J, Kim HI, Bang Y, Choi HJ. Peroxisome proliferator-activated receptor gamma: a novel therapeutic target for cognitive impairment and mood disorders that functions via the regulation of adult neurogenesis. Arch Pharm Res. 2021;44(6):553–63.
28. Huss JM, Garbacz WG, Xie W. Constitutive activities of estrogen-related receptors: Transcriptional regulation of metabolism by the ERR pathways in health and disease. Biochim Biophys Acta. 2015;1852(9):1912–27.
29. Misra J, Kim DK, Choi HS. ERRγ: a Junior Orphan with a Senior Role in Metabolism. Trends Endocrinol Metab. 2017;28(4):261–72.
30. Gofflot F, Chartoire N, Vasseur L, et al. Systematic gene expression mapping clusters nuclear receptors according to their function in the brain. Cell. 2007;131(2):405–18.
31. Hermans-Borgmeyer I, Süsens U, Borgmeyer U. Developmental expression of the estrogen receptor-related receptor gamma in the nervous system during mouse embryogenesis. Mech Dev. 2000;97(1–2):197–9.
32. Tanida T, Matsuda KI, Yamada S, Kawata M, Tanaka M. Immunohistochemical profiling of estrogen-related receptor gamma in rat brain and colocalization with estrogen receptor alpha in the preoptic area. Brain Res. 2017;1659:71–80.
33. Lim J, Choi HS, Choi HJ. Estrogen-related receptor gamma regulates dopaminergic neuronal phenotype by activating GSK3β/NFAT signaling in SH-SY5Y cells. J Neurochem. 2015;133(4):544–57.
34. Kim HI, Lee S, Lim J, et al. ERRγ ligand HPB2 upregulates BDNF-TrkB and enhances dopaminergic neuronal phenotype. Pharmacol Res. 2021:105423.

35. Marras C, Schüle B, Munhoz RP, et al. Phenotype in parkinsonian and nonparkinsonian LRRK2 G2019S mutation carriers. Neurology. 2011;77(4):325–33.
36. Vints K, Vandael D, Baatsen P, et al. Modernization of Golgi staining techniques for high-resolution, 3-dimensional imaging of individual neurons. Sci Rep. 2019;9(1):130.
37. Meijering E, Jacob M, Sarria JC, et al. Design and validation of a tool for neurite tracing and analysis in fluorescence microscopy images. Cytometry A. 2004;58(2):167–76.
38. Lim J, Bang Y, Choi JH, et al. LRRK2 G2019S Induces Anxiety/Depression-like Behavior before the Onset of Motor Dysfunction with 5-HT(1A) Receptor Upregulation in Mice. J Neurosci. 2018;38(7):1611–21.
39. Li X, Patel JC, Wang J, et al. Enhanced striatal dopamine transmission and motor performance with LRRK2 overexpression in mice is eliminated by familial Parkinson's disease mutation G2019S. J Neurosci. 2010;30(5):1788–97.
40. Winner B, Melrose HL, Zhao C, et al. Adult neurogenesis and neurite outgrowth are impaired in LRRK2 G2019S mice. Neurobiol Dis. 2011;41(3):706–16.
41. Höglinger GU, Rizk P, Muriel MP, et al. Dopamine depletion impairs precursor cell proliferation in Parkinson disease. Nat Neurosci. 2004;7(7):726–35.
42. Winner B, Regensburger M, Schreglmann S, et al. Role of α-synuclein in adult neurogenesis and neuronal maturation in the dentate gyrus. J Neurosci. 2012;32(47):16906–16.
43. von Bohlen und Halbach O, von Bohlen und Halbach V. BDNF effects on dendritic spine morphology and hippocampal function. Cell Tissue Res. 2018;373(3):729–41.
44. Spampanato J, Sullivan RK, Turpin FR, Bartlett PF, Sah P. Properties of doublecortin expressing neurons in the adult mouse dentate gyrus. PLoS One. 2012;7(9):e41029.
45. Crespel A, Rigau V, Coubes P, et al. Increased number of neural progenitors in human temporal lobe epilepsy. Neurobiol Dis. 2005;19(3):436–50.
46. Deuel TA, Liu JS, Corbo JC, et al. Genetic interactions between doublecortin and doublecortin-like kinase in neuronal migration and axon outgrowth. Neuron. 2006;49(1):41–53.
47. Tomita S, Nicoll RA, Bredt DS. PDZ protein interactions regulating glutamate receptor function and plasticity. J Cell Biol. 2001;153(5):F19-24.
48. Micheli L, Ceccarelli M, D'Andrea G, Tirone F. Depression and adult neurogenesis: Positive effects of the antidepressant fluoxetine and of physical exercise. Brain Res Bull. 2018;143:181–93.
49. Wang H, Xu J, Lazarovici P, Quirion R, Zheng W. cAMP Response Element-Binding Protein (CREB): A Possible Signaling Molecule Link in the Pathophysiology of Schizophrenia. Front Mol Neurosci. 2018;11:255.
50. Géral C, Angelova A, Lesieur S. From molecular to nanotechnology strategies for delivery of neurotrophins: emphasis on brain-derived neurotrophic factor (BDNF). Pharmaceutics. 2013;5(1):127–67.
51. Shirayama Y, Chen AC, Nakagawa S, Russell DS, Duman RS. Brain-derived neurotrophic factor produces antidepressant effects in behavioral models of depression. J Neurosci. 2002;22(8):3251–61.
52. Shih-Jen T. A Clinical view of BDNF-TrkB signaling in the treatment of major depression. Curr Signal Transduct Ther. 2007;2(3):186–9.
53. Gudasheva TA, Povarnina P, Tarasiuk AV, Seredenin SB. The low molecular weight brain-derived neurotrophic factor mimetics with antidepressant-like activity. Curr Pharm Des. 2019;25(6):729–37.
54. Gudasheva TA, Povarnina PY, Seredenin SB. Dipeptide mimetic of the brain-derived neurotrophic factor prevents impairments of neurogenesis in stressed mice. Bull Exp Biol Med. 2017;162(4):454–7.
55. Zhang JC, Yao W, Dong C, et al. Comparison of ketamine, 7,8-dihydroxyflavone, and ANA-12 antidepressant effects in the social defeat stress model of depression. Psychopharmacology. 2015;232(23):4325–35.
56. Huang Y, Huang C, Zhang Q, Wu W, Sun J. Serum BDNF discriminates Parkinson's disease patients with depression from without depression and reflect motor severity and gender differences. J Neurol. 2021;268(4):1411–8.
57. Horard B, Vanacker JM. Estrogen receptor-related receptors: orphan receptors desperately seeking a ligand. J Mol Endocrinol. 2003;31(3):349–57.
58. Xie W, Hong H, Yang NN, et al. Constitutive activation of transcription and binding of coactivator by estrogen-related receptors 1 and 2. Mol Endocrinol. 1999;13(12):2151–62.
59. Zhang Z, Teng CT. Estrogen receptor-related receptor alpha 1 interacts with coactivator and constitutively activates the estrogen response elements of the human lactoferrin gene. J Biol Chem. 2000;275(27):20837–46.
60. Sohrabji F, Miranda RC, Toran-Allerand CD. Identification of a putative estrogen response element in the gene encoding brain-derived neurotrophic factor. Proc Natl Acad Sci U S A. 1995;92(24):11110–4.
61. Healy DG, Falchi M, O'Sullivan SS, et al. Phenotype, genotype, and worldwide genetic penetrance of LRRK2-associated Parkinson's disease: a case-control study. Lancet Neurol. 2008;7(7):583–90.
62. Belarbi S, Hecham N, Lesage S, et al. LRRK2 G2019S mutation in Parkinson's disease: a neuropsychological and neuropsychiatric study in a large Algerian cohort. Parkinsonism Relat Disord. 2010;16(10):676–9.
63. Beavan M, McNeill A, Proukakis C, et al. Evolution of prodromal clinical markers of Parkinson disease in a GBA mutation-positive cohort. JAMA Neurol. 2015;72(2):201–8.
64. Schrag A, Taddei RN. Depression and anxiety in Parkinson's Disease. Int Rev Neurobiol. 2017;133:623–55.
65. Ben Romdhan S, Farhat N, Nasri A, et al. LRRK2 G2019S Parkinson's disease with more benign phenotype than idiopathic. Acta Neurol Scand. 2018;138(5):425–31.
66. Westerlund M, Belin AC, Anvret A, et al. Developmental regulation of leucine-rich repeat kinase 1 and 2 expression in the brain and other rodent and human organs: Implications for Parkinson's disease. Neuroscience. 2008;152(2):429–36.
67. Piccoli G, Condliffe SB, Bauer M, et al. LRRK2 controls synaptic vesicle storage and mobilization within the recycling pool. J Neurosci. 2011;31(6):2225–37.
68. Qiao H, Li MX, Xu C, et al. Dendritic spines in depression: What we learned from animal models. Neural Plast. 2016;2016:8056370.
69. Kowiański P, Lietzau G, Czuba E, et al. BDNF: A key factor with multipotent impact on brain signaling and synaptic plasticity. Cell Mol Neurobiol. 2018;38(3):579–93.